Chemistry & Biology, Vol. 12, 385–395, March, 2005, ©2005 Elsevier Ltd All rights reserved. DOI 10.1016/j.chembiol.2005.01.015

Screening for Cell Migration Inhibitors via Automated Microscopy Reveals a Rho-Kinase Inhibitor

Justin C. Yarrow,[1,2,*] Go Totsukawa,[3] Guillaume T. Charras,[1] and Timothy J. Mitchison[1,2]
[1]Department of Systems Biology
[2]Institute for Chemistry and Cell Biology (ICCB)
Harvard Medical School
Boston, Massachusetts 02115
[3]Department of Molecular Biology and Biochemistry
Rutgers University
Piscataway, New Jersey 08854

Summary

Small-molecule kinase inhibitors are predominantly discovered in pure protein assays. We have discovered an inhibitor of Rho-kinase (ROCK) through an image-based, high-throughput screen of cell monolayer wound healing. Using automated microscopy, we screened a library of 16,000 compounds finding many that affected cell migration or cell morphology as well as compounds that blocked mitotic progression. We tested 200 compounds in a series of subassays and chose one, 3-(4-pyridyl)indole (Rockout), for more detailed characterization. Rockout inhibits blebbing and causes dissolution of actin stress fibers, phenocopying Rho-kinase inhibitors. Testing Rho-kinase activity in vitro, Rockout inhibits with an IC_{50} of 25 μM (5-fold less potent than Y-27632) but has a similar specificity profile. We also profile the wound healing assay with a library of compounds with known bioactivities, revealing multiple pathways involved in the biology.

Introduction

Cell migration requires the coordination of numerous cellular processes including polarization, actin cytoskeletal reorganization, membrane cycling, and adhesion. One approach to studying this complex phenomenon has come through the use of small molecules which can be used to temporally and spatially regulate individual proteins and processes. Numerous small molecules that are known to inhibit cell migration exist and have been used extensively; however, our ability to perturb specific protein function is limited by the compounds available.

Small molecules that are commonly used to study cell migration have predominantly been discovered through their activity in non-cell migration assays (toxicity and proliferation), rather than by high-throughput screening of the phenomenon itself [1–3]. In recent years, technology development has allowed high-throughput screens that assay cellular and multicellular phenomena, and allow observation of complex phenotypes. These include: G protein-coupled receptor shuttling, protein translocation through the ER and Golgi to the plasma membrane, nuclear translocation, angiogenesis, and progression through the cell cycle [4–6]. These screens are known as phenotypic screens and in an analogy to genetic screens, they aim to discover a small-molecule inhibitor for each protein involved in a process [7]. Cell imaging provides an interesting readout of phenotypic screens. Image-based screens provide detailed information about the process under study and as such are often referred to as high content screens [8–10].

We developed an image-based, high content, cell migration screen in a 384-well format using scratch wound healing as a model system [11]. Using this assay, we screened for compounds that affect wound healing and cell migration. In beginning this work, we had two goals: finding small-molecule tools for in-depth cell biological study and developing technologies for image-based screening. We performed a large phenotypic screen for migration-inhibiting small molecules then took the hits through a series of more detailed assays and molecular characterization. This resulted in the characterization of a small molecule, the identification of its protein target, and the development of a linked series of assays that can be used in future screens of small-molecule, siRNA, and protein libraries.

Results

Screening for Small Molecules that Affect Wound Healing

We developed an assay for finding inhibitors or activators of cell migration using automated microscopy to observe migration of mammalian epithelial cells 7 hr after wounding of a confluent monolayer [11]. In this type of migration assay, cells are thought to respond to increased exposure to serum growth factors at the wound margin by chemotaxis into the open area [12, 13]. We screened library of ~16,000 drug-like small molecules at a nominal concentration of 50 μM, and observed four predominant phenotypes: decreased migration, aberrant morphology of migrating cells, increased number of round cells (found for the most part to be mitotic cells), and compounds that disrupted the cell monolayer (Figure 1A). No activators of migration were observed, presumably because the high serum concentration in our assay maximally stimulated migration. Monolayer disruption was considered a gross indication of toxicity, and compounds with this effect were typically not tested further. Wells often showed a combination of phenotypes (e.g., both inhibition of wound healing and aberrant morphology).

From the initial 16,000 compounds, ~150 compounds decreased migration, ~600 compounds caused aberrant morphology, and ~450 compounds increased the number of mitotic cells. The initial categorization was intentionally broad, and compounds were placed in multiple categories. Removing redundancy, as well as compounds that increased the number of mitotic cells, or caused complete disruption of the monolayer, we were left with ~400 compounds that affected migration or morphology.

*Correspondence: jyarrow@post.harvard.edu

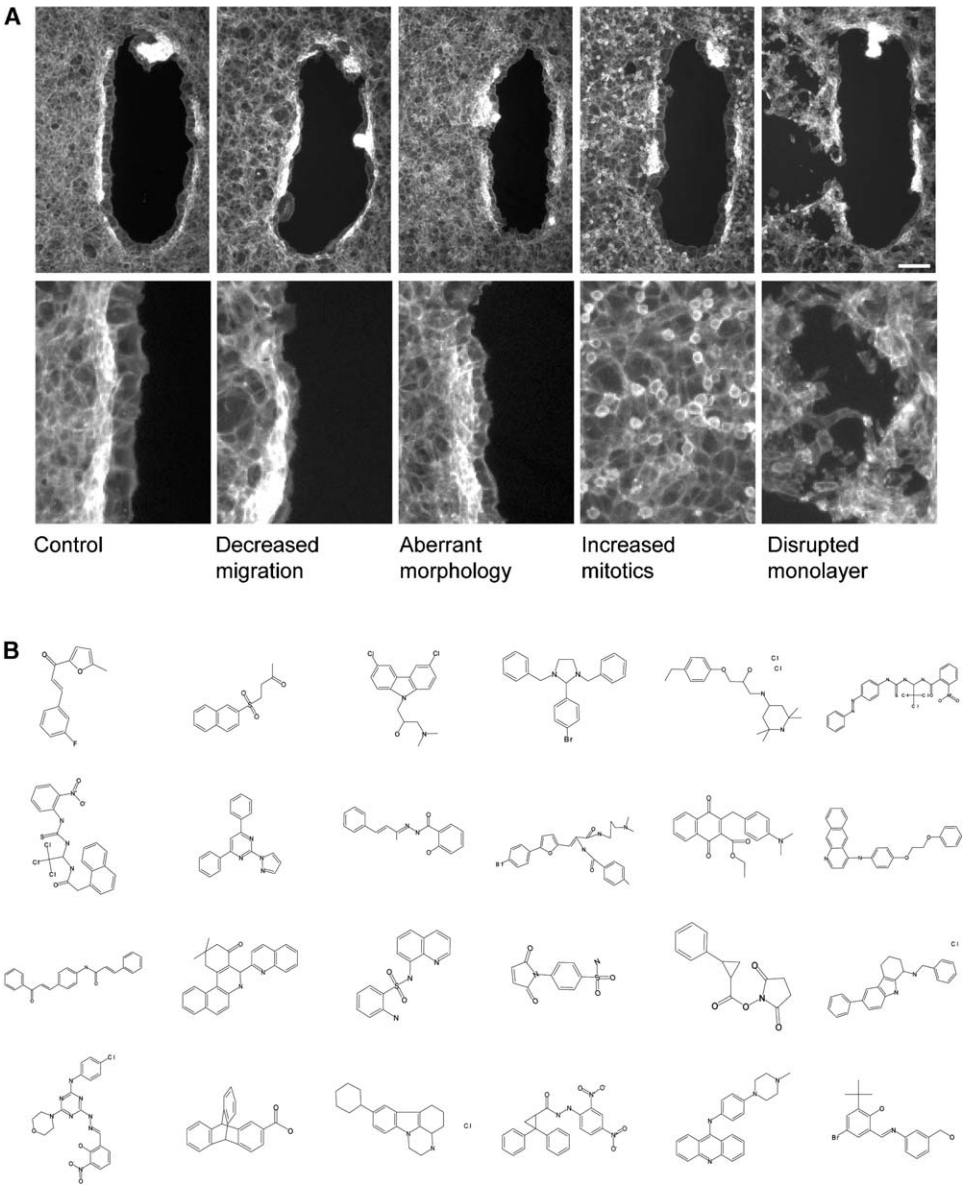

Figure 1. A High-Content Screen for Small Molecules that Affect Wound Healing

(A) The five predominant phenotypes observed in a primary screen for small molecules that affect 7 hr wound healing of BS-C-1 monolayers: normal, decreased cell migration, aberrant cell morphology, increased mitotic cells, and disrupted monolayer (toxic). Cells are stained with phalloidin to visualize filamentous actin.

(B) Compound structures from each of the 24 structural classes found to have an effect in the wound healing assay.

To narrow the number of compounds for subsequent study, we categorized compounds into 24 classes of chemically related molecules by visual inspection of structures (Figure 1B), plus 278 singleton compounds. From each structural class, we chose the compound with the most drastic effect on cells for follow-up, assuming (possibly incorrectly as discussed below) that other compounds in the same class act by the same mechanism, but less potently. From the singletons, we selected compounds on the basis of attractive chemical features, including: multiple heterocyclic rings, nitrogen containing heterocycles, polar groups, expected chemical stability, and lack of chemically reactive functionality [14]. The resulting sublibrary of ~200 active compounds was screened in several other assays, and compared to a database of activities for the larger chemical library. The assay that was most relevant to the wound healing screen was an in vitro screen of Cdc-42-dependent actin polymerization in *Xenopus laevis* frog egg extract [15, 16]. This assay was performed prior to ours and targeted a subset of the processes involved in wound healing. We excluded compounds found to inhibit in both this in vitro assay and ours.

Table 1. Characteristics of the Assay and Subassays

Assay	Assay Type	Minimum Duration Required for Readout	Complexity of Underlying Biology (Subjective Rank)
Wound healing	Multi and single cell	7 hr	1
Phagocytosis	Single cell	~1 hr	2
M2 blebbing	Single cell	10 min	3
Timelapse microscopy	Single cell	10 min	3
Cell spreading after trypsinization	Single cell	~30 min	3
Toxicity	Single cell	10 min	4
Actin polymerization in permeabilized *S. cerevisiae*	In vitro	10 min	5
Listeria-dependent actin polymerization	In vitro	10 min	5

The characteristics described above define a set of assays with overlapping complexity, biochemical accessibility, and rapidity of readout that can be used to subdivide compounds for follow-up. (The subjective ranking is based on the assay type and what is known from observation or the literature.)

Though we removed compounds that increased the number of mitotic cells from further analysis of cell migration effects, these compounds merit further comment. Finding wells with an increased number of mitotic cells was an unexpected bonus in our screen, reflecting the high information content of microscopy images. These wells were restained with an anti-tubulin antibody and inspected at higher magnification. One compound gave a monoaster phenotype and was subsequently shown to inhibit the mitotic kinesin Eg5 [17]. Visual inspection of the other mitotic wells showed either microtubule depolymerization or a phenotype characteristic of a microtubule dynamics perturbation (a smaller mitotic spindle with chromosomes at the poles and throughout the length of the spindle), and a subset of these were confirmed as tubulin polymerization inhibitors in vitro (T. Mayer, personal communication). However, some of the suspected microtubule depolymerizers score differently with respect to inhibiting migration, suggesting that some compounds may target other proteins involved in microtubule dynamics, or target tubulin as well as another process.

Secondary Assays Define One Compound, Rockout, for Follow-Up

With approximately 200 compounds in hand, we developed a series of secondary assays to narrow the number of compounds further and to profile their biological activity. We were particularly interested in finding compounds that affected proteins and processes involved in the regulation of the actin cytoskeleton, but we didn't want to limit ourselves to these processes. We therefore selected secondary assays that were sensitive to small-molecule inhibitors of the actin cytoskeleton yet were significantly complex that inhibition of other processes would manifest in the assays. Other major considerations in choosing subassays were the rapidity of the readout of an assay and developing a set of assays that monitored overlapping and complementary processes (Table 1). Assays with rapid readouts were chosen to select compounds that affect the dynamic aspects of an assay rather than those aspects that took hours to manifest, e.g., changes in transcription and translation. The range of assays—from complex, in vivo, to simpler, in vitro, assays—was chosen with the hope that some compounds would inhibit in both types of assays and thus select for compounds that were potentially specific. The use of overlapping assays would also narrow the number of potential targets (from many in an in vivo assay to fewer in an in vitro assay) and provide a route to target identification via biochemical methods (Table 1). We used the following assays: IgG mediated phagocytosis of *E. coli* by macrophages, cell spreading, cell blebbing, observation of cellular effects by time-lapse microscopy, actin polymerization in permeabilized *S. cerevisiae*, in vitro *Listeria monocytogenes* motility, and toxicity measured by membrane permeability and ATP levels (Figure 2A) (see Experimental Procedures for details).

From our 200 active compounds, we found inhibitors that were active in each subassay except *Listeria* motility and actin polymerization in permeabilized yeast; however, nearly all compounds showed undesirable effects, including: toxicity after 24 hr treatment (some were toxic after 7 or 2 hr; data not shown), vacuolization of cells when observed by transmitted-light microscopy, or insolubility at low concentrations.

One compound that was not toxic, promoted cell spreading, and inhibited blebbing, was 3-(4-pyridyl)indole (Rockout) (Figure 2B). Rockout initially scored as a compound that caused decreased migration and aberrant morphology. A dose-response series shows a distinct effect in the wound healing assay at 50 μM (Figure 2C). Rockout did not affect phagocytosis, *Listeria* motility or actin polymerization in permeabilized yeast.

Rockout Inhibits Blebbing and Leads to Dissolution of Stress Fibers

Rockout was chosen for follow-up after observing that treatment inhibited blebbing of recently trypsinized Swiss3T3 cells (data not shown)—an effect that was not observed with any of the other compounds tested and was intriguing given what is known about the role of the actin cytoskeleton in the phenomenon of blebbing [18–21]. We observed the same effect when testing Rockout on blebbing using M2 cells, a human melanoma cell line that blebs constitutively in a manner that is sensitive to actin cytoskeletal perturbation [19–23]. When Rockout was added at 50 μM, M2 cells stopped blebbing within 2 min and with washout blebbing returned to normal levels within 3 min (Figure 3A).

Monitoring blebbing of M2 cells is a robust, rapid as-

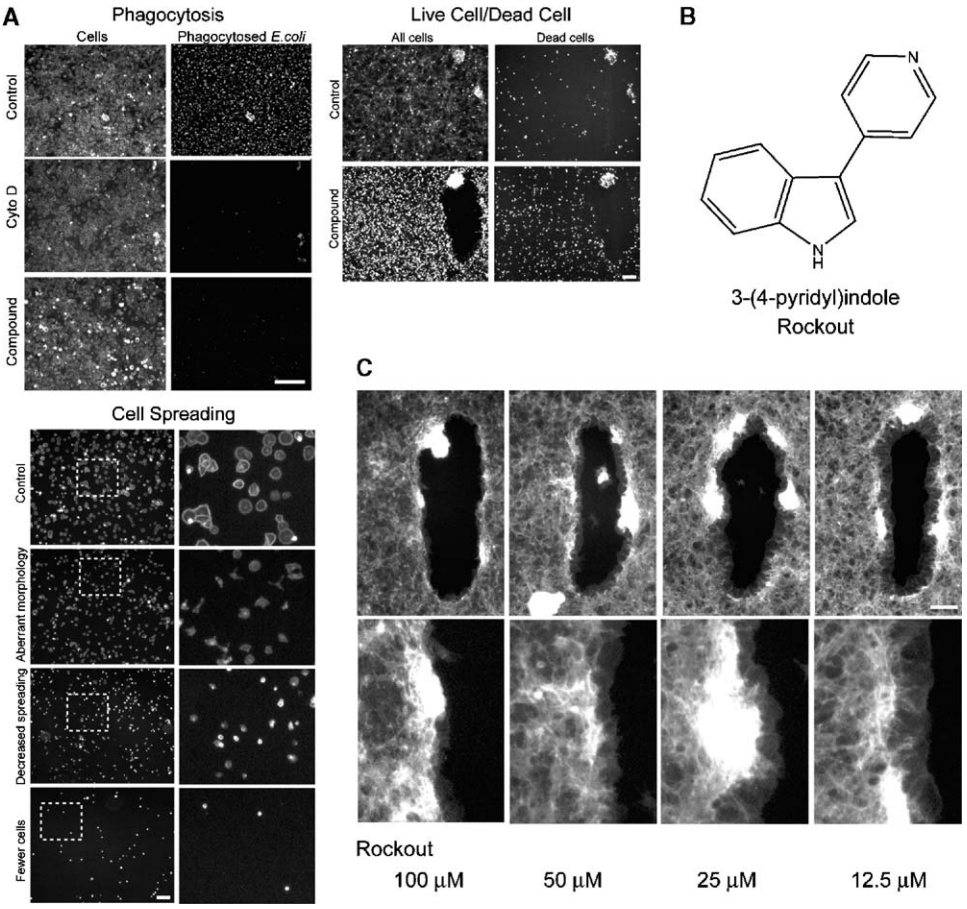

Figure 2. Secondary Assays Lead to Rockout for Follow-Up

(A) Three of the secondary assays used to narrow the compounds found in the wound healing screen—phagocytosis, cell spreading, and live cell/dead cell. The phagocytosis assay shows a compound with normal phagocytosis, the effect of cytochalasin D, and a compound that blocked phagocytosis but showed balled and brightly staining cells which suggest toxicity. The cell spreading assay found compounds that had no effect on spreading, led to spreading with aberrant morphology, allowed adherence but not spreading, and led to fewer cells adhering. A live cell/dead cell assay 24 hr after wounding. DMSO treatment shows complete healing after 24 hr (live cells stained with calcienAM) and minimal dead cells (ethidium homodimer staining is minimal). A compound that blocks wound healing after 24 hr shows increased toxicity.

(B) The structure of Rockout, 3-(4-pyridyl)indole, chosen for follow-up studies after performing subassays.

(C) Titration of Rockout in the wound healing assay shows that it has a distinct effect on morphology at 50 μM.

say that allowed us to quantify the effect of Rockout and its derivatives. Inhibition of blebbing by Rockout can be easily seen after fixation and staining for filamentous actin (Figure 3B). To determine an IC_{50} for Rockout, we treated cells for 10 min with a dilution series before staining and counting cells with blebs. We found that Rockout has an IC_{50} of ~12 μM (Figure 3B) and it inhibits blebbing in nearly all cells at 50 μM—the concentration used for subsequent experiments. To begin to establish a structure-activity relationship, we tested two derivatives of Rockout and a control compound with similar chemical characteristics. We found that RD2 had a dose response similar to Rockout, RD3 had almost no effect at up to 100 μM, and RD4 also had no effect (Figure 3B). RD3 and RD4 had no effect on longer incubation in time-lapse microscopy experiments (data not shown). These structure-activity studies reveal the importance of one of the heterocyclic nitrogens, and point to a site for future chemical modification to increase potency.

Balb 3T3 (B3T3) cells, a fibroblast cell line, have well defined actin structures, and we used them to investigate the specific effect of Rockout on the actin cytoskeleton. Treatment of B3T3 cells with 50 μM Rockout leads to significant morphological change within 10 min in a manner that suggests changes in contractility or adhesion (Figure 3C). Cells do however continue to ruffle, suggesting leading edge activity (which is dependent on rapid actin polymerization) is normal. We fixed and stained cells for filamentous actin after treating with 50 μM Rockout for 10 min. Cells treated in the presence of serum showed decreased stress fiber staining, and this effect was more easily observed after overnight serum starvation followed by Rockout treatment (Figure 3D). Localization of the stress fiber and focal adhesion complex proteins α-actinin, filamin, vinculin, and ezrin, were also disrupted by the Rockout treatment (data not shown).

ROCK Is a Molecular Target of Rockout

Given the effect of Rockout on cell morphology, stress fibers, and blebbing, we suspected that it might be act-

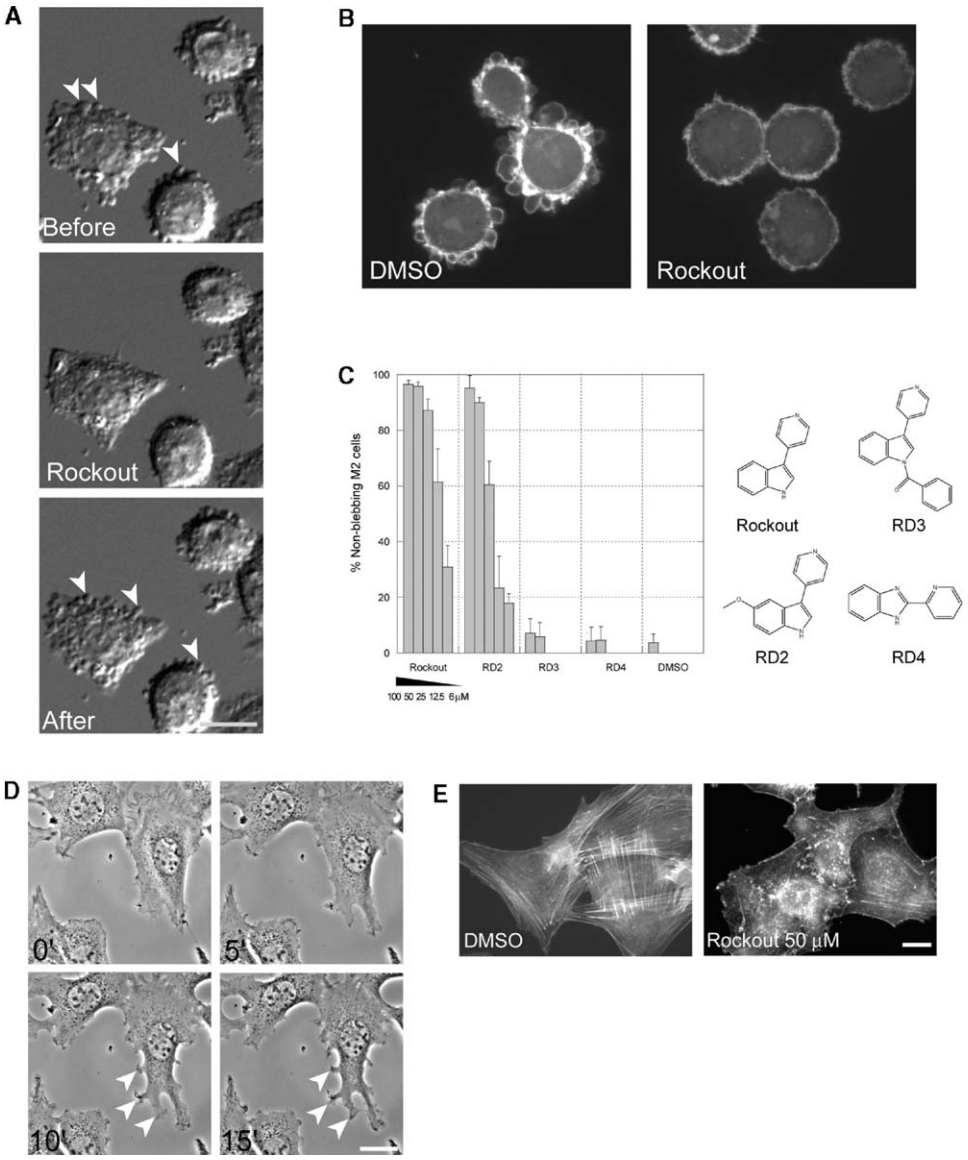

Figure 3. Rockout Inhibits Blebbing in M2 Cells and Leads to Stress Fiber Disassembly

(A) Constitutively blebbing M2 cells stop blebbing within 2 min after the addition of 50 μM Rockout and return to normal levels within 3 min after washout. Arrows note prominent blebs.

(B) High magnification images of the phenotypes used in quantifying the effect of Rockout and derivatives below. Fixed and stained for filamentous actin after 2 min, cells show blebs in DMSO and do not in 50 μM Rockout.

(C) A Rockout dilution series (100, 50, 25, 12.5, and 6 μM) shows that Rockout blocks blebbing in all cells at 50 μM and has an approximate IC_{50} of 12 μM. RD1 inhibits blebbing with a similar IC_{50} while RD3 and RD4 have little or no effect. M2 cells were treated with a dilution series of the compounds noted for 10 min, fixed, stained, and counted.

(D) Balb 3T3 cells treated with 50 μM Rockout show effects within 10 min that are consistent with perturbation to contractility or adhesion. Arrows note ruffling protrusions following contraction.

(E) Serum-starved cells treated with 50 μM Rockout for 10 min show loss of stress fibers compared to DMSO treatment.

ing in the Rho pathway. Treatment with Y-27632, a small-molecule inhibitor of Rho kinases (ROCKI and ROCKII, hereafter ROCK), leads to stress fiber dissolution, affects cell morphology, and inhibits blebbing [20, 24–27]. We found that the effect of 50 μM Rockout was equivalent to that of 10 μM Y-27632 on stress fiber dissolution, and subsequent experiments used these concentrations, respectively (data not shown). We directly investigated the effect of Rockout on the Rho signaling pathway, using myosin light chain (MLC) phosphorylation as a readout. Rho-kinases are serine/threonine kinases that are activated by Rho [28]. Upon activation of the Rho pathway, ROCK interacts with and phosphorylates downstream effector proteins, including myosin light chain [29–31]. To test for an effect on MLC phosphorylation, we starved M2 and B3T3 cells overnight, incubated with compounds for 10 min, stimulated with serum or not, and harvested after 10 additional minutes. Using an antibody specific to phosphorylation of MLC at Ser19, we found that, in both the presence and absence of serum, Rockout and Y-27632 caused a similar decrease in phosphorylation levels (Figure 4A). To de-

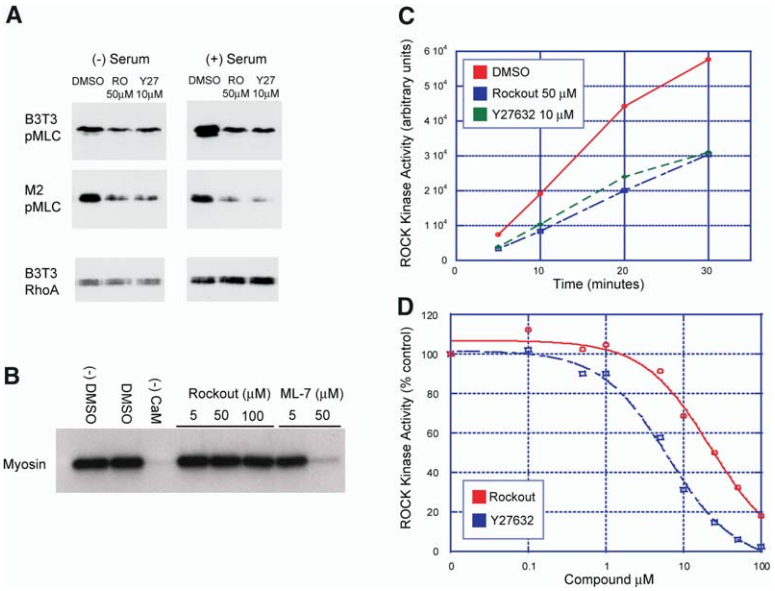

Figure 4. Rockout Inhibits ROCK in a Manner Similar to Y-27632

(A) Rockout and Y-27632 block myosin light chain phosphorylation in Balb 3T3 cells and M2 cells but do not block Rho activation. Representative Western blots of cell lysates after treatment with DMSO, 50 μM Rockout (RO), or 10 μM Y-27632 with or without serum stimulation.

(B) MLCK in vitro activity is not inhibited by Rockout at concentrations up to 100 μM but is inhibited by the MLCK inhibitor ML-7 or by the absence of calmodulin (CaM) in the assay.

(C) Rockout inhibits ROCK in vitro activity at 50 μM in a manner similar to 10 μM Y-27632.

(D) Titration of Rockout and Y-27632 shows an approximate IC_{50} of 25 μM for Rockout and 5 μM for Y-27632 as measured in this assay.

termine where in the Rho pathway Rockout acts, we treated B3T3 cells as above, and assayed Rho activation by a pull-down assay with immobilized Rho binding domain (RBD) from Rhotekin [32]. Rockout did not inhibit Rho activation (Figure 4A), showing that it acts below Rho in the pathway.

Myosin light chain is primarily phosphorylated by both myosin light chain kinase (MLCK) and ROCK. To test the effect of Rockout on MLCK activity, we performed in vitro kinase assays using human platelet myosin as substrate. Rockout did not affect phosphorylation by MLCK (up to 100 μM) while the MLCK inhibitor ML-7 blocked phosphorylation at 50 μM (Figure 4B).

We next tested directly if Rockout inhibits ROCK activity. Performing kinase assays with purified ROCK catalytic domain [29] and myelin basic protein as substrate, we found that 50 μM Rockout inhibits ROCK in a manner similar to 10 μM Y-27632 (Figure 4C). A dose response of Rockout and Y-27632 showed an approximate IC_{50} of 25 μM for Rockout and 5 μM for Y-27632 at an ATP concentration of 100 μM (Figure 4D). Y-27632 is a competitive inhibitor, competing with ATP [33], and preliminary experiments with Rockout show that it is also competitive with ATP (data not shown).

Rockout Kinase Specificity

Small-molecule inhibitors often have multiple targets, and this is especially likely to be true for ATP-competitive kinase inhibitors, given the conserved nature of kinase active sites. Our pathway analysis already demonstrated that Rockout is not a nonspecific kinase inhibitor. Phosphorylation of AKT and ERM proteins and phosphotyrosine levels in response to serum addition were also unaffected (Figure 5A). To test Rockout's specificity we assayed its effect on five other kinases in vitro. Using a concentration of 25 μM (our measured in vitro IC_{50}), we tested kinases that have been shown to be inhibited by Y-27632, and other ROCK inhibitors, as well as kinases that are not inhibited by these compounds [34]. As seen in Figure 5B, 25 μM Rockout inhibits ROCK-II and PRK2, another Rho-dependent kinase, to a similar degree, and MSK-1 and PKA to a lesser extent (Figure 5B). Rockout does not inhibit PKCα or SAPK2a. In a profiling study of numerous kinase inhibitors, the compound H-89 inhibited ROCKII, PKA, S6K1, and MSK1 with similar potency [34]. Thus, we have found a ROCK inhibitor with 5-fold lower potency than Y-27632 when tested in vitro and a specificity profile that is most similar to the ROCK inhibitor H-89.

Profiling the Wound Healing Assay Using Compounds with Known Bioactivities

We were also interested in determining the possible targets of the other compounds discovered from our screen. Compounds with established bioactivities can be used in this respect to determine how a biological assay responds to a wide array of known perturbations and in this way reveal potential small-molecule targets. Such compounds come with caveats; they might have multiple targets and some of those targets might not be known. However, small molecules with known activities can focus attention on particular pathways, including those that would not otherwise be considered.

We screened a library of ~500 compounds with known bioactivities at three concentrations in the 7 hr wound healing assay. These compounds were selected from commercial sources to cover a wide range of targets and processes and similar collections are now commercially available (for a complete list, see the link in Experimental Procedures). After screening in duplicate, wells that differed significantly from the control phenotype were categorized by visual inspection, as per our original screen. We then assigned each compound a number from 1 to 3 (highest to lowest) that reflected the strength of the phenotype. Compounds that were toxic at the lowest concentration and compounds that clearly increased the number of mitotic

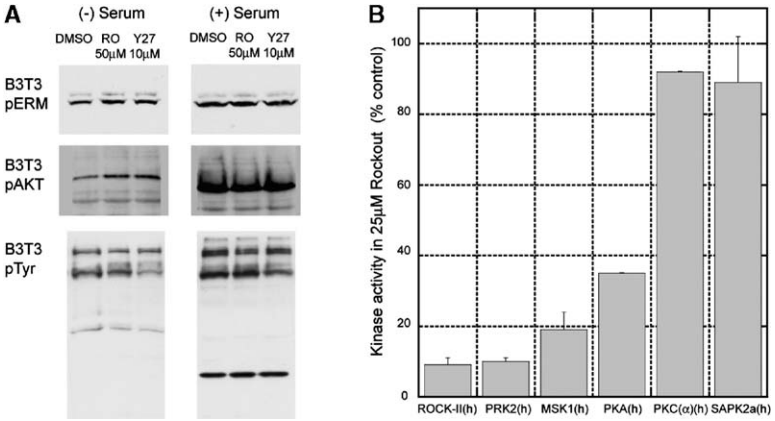

Figure 5. Rockout Has Similar Specificity to Other ROCK Inhibitors

(A) Rockout has no effect on pAKT, pERM, or pTyr levels. Representative Western blots of cell lysates after treatment with DMSO, 50 μM Rockout (RO), or 10 μM Y-27632 with or without serum stimulation.

(B) Testing other kinases with 25 μM Rockout in vitro, we find that Rockout has a specificity profile similar to the ROCK inhibitor H-89, inhibiting ROCKII, MSK1, and PKA.

cells were automatically ranked 3. Though subjective, visual inspection reveals compounds and phenotypes that do not fit the parameters of a defined automated analysis and as such is more inclusive [11]. Out of 489 compounds, we found 37 that consistently affected migration (Figure 6A) and 12 that primarily affected morphology (Figure 6B). A complete dataset, including images, is available upon request.

Profiling with known bioactives, we found many expected compounds, such as the actin disrupting drugs cytochalasin D, jasplakinolide, and latrunculin B. Others were less expected, such as the CDK inhibitor alsterpaullone and the kinase inhibitor rottlerin (Figure 6). To determine how the compounds might be affecting wound healing, we compiled the published mechanism of action of all 489 compounds. We then categorized

A

Predominantly affect migration

Compound	Strength	Phenotype	Conc.	Target Cat.	Compound targets/processes
Alsterpaullone	1	decreased mig	H,M,L		Inhibits Cdks
Latrunculin B	1	no mig, cytoD	H,M,L		Inhibits F-Actin
PP1	1	lamella okay, delayed migration	H,M,L		Inhibits p60src, Inhibits p59fyn, Inhibits v-src
cytochalasin D	1	no mig, cytoD	H,M,L		Inhibits F-Actin
wortmannin	1	decreased mig	H,M,L		Inhibits; Map kinase (non specific), MLCK, Phospholipase D,Pi 4 kinase, PI3Kinase
ouabain	1	decreased mig	H,M,L		Inhibits Na+/K+ ATPase
Go6976	1	decreased mig	H,M		Inhibits PKC
jasplakinolide	1	no mig, low stain	H,M		F-Actin
K252c	1	decreased mig, morph	H,M		Inhibits PKA, Inhibits PKC
menadione	1	no migration, tox? at High	H, M		Oxydative stress
LY83583	1	no mig, interesting ML	H		Inhibits Ca2+i, Inhibits cGMP, Inhibits Guanylate cyclase
okadaic acid	1	dec. mig, mitotics?, very aberrant morph	H		Inhibits PP1, Inhibits PP2A
Rottlerin	1	decreased mig, lamella okay	H		Inhibits cAM kinase, Inhibits PKC
LY294002	1	no migration	H		Inhibits PI3Kinase, Inhibits Proliferation
Curcumin	1	decreased mig, morph	H		Inhibits Cyclooxygenase, Inhibits EGF- RTK, Inhibits iNOS, Inhibits Lipoxygenase
cypermethrin	1	no mig	H		Inhibits Calcineurin, PP2B
methyladenine [3-methyladenine]	1	decreased mig	H		Inhibits CHPI3Kinase
FCCP	1	decreased mig, morph	H		Apoptotic, Cytochrome C, Inhibits Mitochondrial function, Inhibits Mitochondrial ion balance
ethylmaleimide(N)	1	decreased mig	H		Inhibits Apoptotic, Arachidonate, Phospholipase D
isobutyl(3)1methylxanthine	1	decreased mig, morph	H		Inhibits Ca2+i, Inhibits cNdiesterase, cAMP, cGMP, Inhibits; Phosphodiesterase, Purinergic channels
cyclosporin A	1	decreased mig	H		Apoptotic, Inhibits Calcineurin, PP2B, Inhibits NO, Inhibits TNF-alpha
anisomycin	2	decreased mig	H,M,L		Inhibits JNK inhibitor, Inhibits Protein Translocation, SAPK2/p38
dimethylaminopurine (6)	2	decreased mig	H,M,L		JNK inhibitor, Inhibits Non specific kinase inhibitor, Inhibits; PKA, PKC, PKG, Proliferation, TNF-alpha
OBAA	2	decreased mig, nuclear migration defect	H,M		Inhibits PLA2
ANTIBIOTIC A-23187	2	decreased mig	H		Apoptotic, Ca2+i, Inhibits Mitochondrial ion balance
PROSTAGLANDIN A2	2	decreased mig, morph	H		PPAR
tunicamycin	2	decreased mig, morph	H		Inhibits Glycosilation
PD169316	2	decreased mig	H		Inhibits Apoptotic, Inhibits p38 MAPK
AG1478	2	decreased mig, morph	H		Inhibits EGF- RTK, Inhibits PDGF
quercetin	2	decreased mig	H		Inhibits; Mitochondrial ATPase, Phosphodiesterase, PI3Kinase, PKC, PLA2
BW-B 70C	2	decreased mig	H		Inhibits Lipoxygenase
capsazepine	2	decreased mig	H		Capsaicin antagonist, affects ion flux
W7	2	decreased mig	H		Inhibits Calmodulin, Inhibits MLCK
CGP-37157	2	decreased mig	H		Ca2+i, Inhibits Mitochondrial function, Inhibits Mitochondrial ion balance, Inhibits VA - Ca2+ Channel
3-Bromo-7-nitroindazole	2	decreased mig	H		Inhibits iNOS, Inhibits NO
MCI186	2	decreased mig	H		Inhibits Free radicals
dexamethasone	2	decreased mig	H		Apoptotic, Inhibits Cdks, Na+ i, Na+/K+ ATPase, Inhibits NO

Target categories
- Homeostasis
- Signalling
- Cytoskeleton
- Cell cycle

B

Predominantly affect morphology

Compound	Strength	Phenotype	Conc.	Target Cat.	Compound targets/processes
staurosporine	1	very aberrant, moph	H,M,L		Inhibits cAM kinase, Inhibits MLCK, Inhibits PKA, Inhibits PKC, Inhibits PKG
phorbol 12 myristate 13 acetate	1	very aberrant, morph	H,M,L		Apoptotic, Ca2+i, cAMP, iNOS, PKC
H-89	1	very aberrant, morph	H,M,L		Inhibits cAM kinase, Inhibits Casein kinase, Inhibits MLCK, Inhibits PKA, Inhibits PKC, Inhibits PKG
C8 CERAMIDE	1	very aberrant, morph	H,M		Apoptotic, Map kinase (non specific)
THROMBOXANE B2	1	very aberrant, morph	H,M		Thromboxane
HA1077	1	morph	H		Inhibits MLCK, Inhibits PKA, Inhibits PKG, Inhibits Rho kinase
chelerythrine	1	morph	H		Apoptotic, Inhibits PKC
D12-PROSTAGLANDIN J2	1	very aberrant, morph	H		Stimulates gene transcription
blebbistatinMP	1	morph	H		Inhibits Myosin ATPase
brefeldin A	2	morph	H,M		Inhibits Cholesterol, Inhibits Protein Translocation
NIGULDIPINE	2	morph	H		Inhibits Ca2+i
roscovitine	2	morph, cells leaving monolayer	H		Inhibits Cdks, Inhibits ERK, Inhibits Proliferation

Figure 6. Compounds with Known Bioactivities that Affect Migration and Morphology in the Wound Healing Assay

(A) Compounds that predominantly affect cell migration.

(B) Compounds that affected cell morphology but not migration.

For both, the column designations that are not self-explanatory are: Strength, the severity of the compound's effect on a decreasing scale from 1 to 3 (only 1 and 2 are shown); Conc., the concentration, high, medium, or low, at which a phenotype was observed; Target Cat., classification of the targets of the small molecules.

the activities of those target proteins and processes and show the highest (most encompassing) level of classification. These are defined as homeostasis, signaling, cytoskeleton, and cell cycle. As expected with a broad phenotypic screen, compounds that affect core cell physiology, such as ion homeostasis and membrane integrity, were found to inhibit in the assay. Interestingly, there were a significant number of compounds that affect the actin cytoskeleton and compounds that target specific signaling cascades suggesting that the proteins and pathways listed in Figure 6 are targets of compounds found with the wound healing assay.

Discussion

We have used a broad phenotypic screen to characterize a small molecule, Rockout, found one of its protein targets, ROCK, and developed a series of subassays for the discovery of small molecules that affect the actin cytoskeleton. Beginning with a high-content image-based screen of scratch wound healing, we found a number of small molecules that decreased cell migration, affected cell morphology of migrating cells, or increased the number of mitotic cells. We categorized these compounds based on chemical characteristics and chose a subset for screening in subassays of specific and general aspects of cell physiology. From these subassays, we chose one compound, Rockout, for follow-up studies. Rockout blocks blebbing in M2 cells and decreases stress fibers in Balb 3T3 cells. Biochemically, Rockout decreases myosin light chain phosphorylation levels, an effect that is also seen with the ROCK inhibitor Y-27632. Testing the predominant kinases that phosphorylate myosin light chain, we found that Rockout does not affect myosin light chain kinase (MLCK) activity but does directly inhibit ROCK.

Our most concrete achievement in this work was to identify a potentially useful inhibitor-protein pair, Rockout-ROCK. Kinases are among the most important targets for therapeutic drug discovery, and the normal route to finding them is pure protein screening. Our data illustrates that phenotypic screening can also be used to discover kinase inhibitors, and in general we believe automated microscopy will be a useful tool for phenotypic characterization in kinase drug discovery programs. Further experiments will be required to explore Rockout's utility as a reagent. Rockout is less potent than the existing ROCK inhibitors Y-27632, H89, and HA1077, but its specificity appears to be comparable. Rockout is a low molecular weight (194.2) and hydrophilic (logP calc = 2.5 ± 0.3) compound making it "lead-like" in its physical properties [35, 36]. These are reasonably impressive characteristics for a compound straight out of a screen, and our structure-activity data show that Rockout can be modified without losing activity, suggesting that more potent derivatives could be synthesized. Human ROCKs are considered potential targets for therapeutic drug development, for example in vascular disease [37, 38], so a heterocyclic scaffold for ROCK inhibitors is potentially useful.

Rockout was only one of many bioactive compounds we identified, because our phenotypic screen covered a broad range of target proteins and processes. An unexpected bonus was identification of useful inhibitors of cell division [17], demonstrating the utility of the high information content inherent in cell imaging. The wound healing assay could be made more specific for finding compounds involved in cell migration by modification of the screen itself, or by use of baseline assays to eliminate compounds that have global effects on cell physiology. For example, the screen could be converted into a differential screen, by comparing wound-migration responses to different trophic factors, or by comparing responses of different cell types to the same trophic factor. It could also be converted into a screen of migration enhancers by using suboptimal concentrations of trophic factors or serum. As an alternative, undesirable compounds could be eliminated from further study by extensive baseline assays. Our use of toxicity assays proved to be highly informative; a number of other baseline assays, such as assays for transcription/translation inhibitors, might similarly be employed in future screens. The results of the screen were also greatly influenced by the initial criteria used for defining interesting hits. The assumption that the compound with the most drastic effect within a structural class was the most potent compound of that class was probably incorrect as we and others have found that these compounds have a very sharp transition from toxic effects to no effect (T. Mayer, personal communication). Another criterion used was toxicity after 24 hr. In retrospect, this is too stringent a criterion for compounds that will be used as tools for cell biological study. Effects observed at 24 hr are not necessarily indicative of, or relevant for, use in a 1 hr or 10 min assay.

As a side benefit of this work, the complexity of cell migration necessitated the development of a number of secondary assays for specific actin-based processes. These assays are not a definitive roadmap for small-molecule discovery of compounds that affect cell migration—they conspicuously ignore aspects of adhesion and do not actively test different signaling cascades—but they do suggest general characteristics for the development of a set of assays that can be used to narrow and profile compounds found from a broad phenotypic screen. Many of these assays can themselves be adapted for high-throughput screening. For example, both the phagocytosis and blebbing assays can easily be performed in multi-well format and, as very dynamic processes, allow readouts in a short time—1 hr and 10 min, respectively. Phagocytosis and blebbing are good assays in part because they manifest the behavior of the highly plastic actin cytoskeleton in discrete and definable ways. And though these assays are susceptible to compounds with global effects, phagocytosis can be monitored throughout the process to determine which step is inhibited (reviewed in [39]) and the process of blebbing consists of discrete molecular events that define bleb formation, size, and retraction (G.T.C., unpublished result). In fact, phagocytosis has been used in a medium throughput format [40] and we have used blebbing as an assay for screening a library of compounds with known bioactivity and have found numerous compounds that had not previously been known to inhibit blebbing (G.T.C., unpublished data).

With the completion of this phenotypic screen, we

are left with a better sense of what phenotypic screens can contribute to the discovery of small molecules. They can be used, as here, to capture the broad array of biological processes that feed into and affect a given process. They can also be tailored to answer narrowly defined and specific questions; for example, by screening for differential effects we might gain insight into differences between cell types that migrate collectively as sheets rather than as individual cells. In both cases, there is a balance between the breadth of potential targets and one's ability to determine the specific target of a given small molecule. To help better define the utility of a phenotypic screen and the compounds discovered with it, initial profiling of an assay with a broad set of small molecules with known bioactivities can provide a sense for the biological processes that could be targets within the screen. Then, once hits have been found, the use of baseline and secondary screens can decrease the number of compounds that inhibit the assay via undesired pathways while subdividing compounds for follow-up.

Significance

We have demonstrated that an image-based screen of a broad biological problem can be used, with appropriate follow-up, to discover interesting ligand-target protein pairs that are relevant to both basic cell biology and therapeutic drug discovery. In the future it will be important to find more small molecules that specifically target proteins involved in cell migration, and variants of the screen and subassays we describe should be useful for this.

Experimental Procedures

Tissue Culture

BS-C-1, Balb 3T3, and J774A.1 cells (ATCC: CCL-26, CCL-163, TIB-67) were grown in DMEM, 4.5 g/l glucose, 10% FCS, with antibiotics. M2 cells were grown in MEM with Earl's salts, 8% calf serum, 2% FBS, 10 mM HEPES (pH 7.5), and antibiotics. All cell lines were maintained at 37°C, 5% CO_2.

Screening of Compound Libraries

As described [11], 384-well clear-bottom plates were seeded with BS-C-1 cells at a concentration of 8500 cells/well in 30 μl of media and incubated overnight. Compound library plates (Chembridge DiverSet E) were thawed and individual assay plates were wounded immediately (within 3 min) with a 96-well pin-transfer device before transfer of compounds. Pin transfer of compounds was accomplished using a robot (Seiko D-TRAN XM3106-31 PN 4-axis cartesian robot) with a 384 pin transfer (transfer volume of 100 nl) (VP Scientific and http://iccb.med.harvard.edu/screening/technology_screen_facil/pin_array_technology.htm). Based on the average molecular weight, compounds were screened at an approximate concentration of 50 μM. Plates were incubated for 7 hr before fixing and staining.

Fixation and Imaging of Screening Plates

Media was removed and permeabilization/fixation (perm/fix) solution (100 mM K-Pipes [pH 6.8], 10 mM EGTA, 1 mM $MgCl_2$, 0.2% Triton X-100, and 3.7% formaldehyde) was added as 30 μl and incubated for 15 min. Wells were aspirated, washed 2 times with TBS containing 0.1% Triton-X 100 (TBS-Tx), and stained with 15 μl TBS-Tx containing 0.5 μg/ml TRITC-phalloidin (Sigma P1591) and 0.1 μg/ml Hoechst (Sigma B2261) for 15 min. Wells were washed 2 times with TBS-Tx and imaged. All liquid handling was done with a wand aspirator (VP scientific VP-186L) and a Labsystems Multidrop.

Imaging and Visual Inspection of Compound Effects

Described in detail in [11]. In brief, individual wells were imaged at 4× using an automated microscope. Images were captured and compiled for visual inspection. Visual analysis of 1 plate of images (384) took 10 min.

Phagocytosis

J774A.1 cells were seeded in 384-well clear bottom plates (as above) at a density of 12,000 cells/well in 45 μl of media and incubated overnight. Compounds were pin transferred or added in 5 μl of media, briefly spun in a tabletop centrifuge (Sorval RT7 plus) for 30 s at 500 rpm, and incubated for 30 min. Fluorescent *E. coli* (Molecular Probes V-6694) were diluted as per instruction in Hank's balanced buffer salt solution. 0.5 μl of diluted *E.coli*, were added to each well in 5 μl of media. Plates were spun for 5 min at 1500 rpm in a tabletop centrifuge (a critical step for consistent results) and incubated for 1 hr. Media were removed and replaced with bromophenol blue (Gibco 15250-061). Fluorescence was measured using a plate reader (Wallac Victor^2) and plates were visually inspected on an inverted microscope before images were taken with the automated microscope with FITC and Rhodamine channels to measure phagocytosis and toxicity (via cell permeability) respectively. Wells showing a decrease of fluorescence levels of 33% relative to the control were noted, as were compounds that caused a noticeable decrease in FITC fluorescence when observed by eye or an increase in the percentage of cells that were fluorescent in the Rhodamine channel.

Cell Spreading

Trypsinized Swiss 3T3 or BS-C-1 cells were added as 4500 cells in 50 μl to a 96-well plate. Fifty microliters of media containing 1 μl of compound or DMSO was added to the wells and the plates were spun in a tabletop centrifuge at 500 rpm for 30 s then incubated for 50 or 75 min. Plates were analyzed by visually inspecting wells and noting phenotypes prior to fixation as well as after fixation and staining (fixed by adding 100 μl of perm/fix solution containing 8% formaldehyde and stained for actin and DNA as above). Compounds that increased or decreased spreading as compared to DMSO were noted, as were compounds that affected the morphology of unspread or spread cells.

Permeabilized Yeast Actin Assembly

Permeabilized yeast actin assembly reactions were performed as described [41, 42] with the modification that permeabilized cells were not urea inactivated. Compounds, tested at 50 μM, were added with extract to the permeabilized cells and again during actin polymerization. The percentage of cells incorporating labeled actin was noted—no compound treatment decreased actin incorporation below the control value of 50%.

Listeria-Dependent Actin Polymerization

Listeria reactions were tried in multiple formats including tail formation in total bovine brain extract and in a two-component system both described in [43]. All compounds tested showed normal tail formation as compared to DMSO except one compound that blocked tail formation but allowed cloud formation. This compound was inconsistent and was dropped from further study.

Time-Lapse Microscopy

Cells were seeded on 25 mm coverslips and adhered for 2 or more hours before imaging. Coverslips were placed in an open-faced chamber warmed to 37°C with 2 mls of media. Cells were treated by removing half of the media from the chamber, mixing it with the compound in an Eppendorf tube, and returning the media to the chamber. Washouts were performed by at least 3× replacement of existing media. With pretreatment and washout, DMSO concentration was kept constant. A compound that showed any effect to

cells that differed from DMSO addition—decreased or increased ruffling, rounding, or morphological changes—was noted.

Toxicity

Cell Titer ATP Assay (Promega G7571)

BS-C-1 cells were plated in 384-well clear-bottom plates overnight at a density of 2000 cells/well in 25 μl. One microliter of compound was added in 25 μl of media to the wells and mixed. At time points of 2 hr and 7 hr, 50 μl of cell titer solution was added. Plates were measured on a plate reader (Wallac) after 2 min of shaking and 8 min incubation. Compounds that showed a 20% decrease in fluorescence relative to the control were noted as toxic.

Live Cell/Dead Cell Assay (Molecular Probes L7010)

BS-C-1 cells were plated in 384-well clear bottom plates overnight as above for wound healing assays. Compounds were added in 5 μl of media to 45 μl and incubated for 2 hr, 7 hr, or 24 hr with or without wounding. Ethidium homodimer and calcienAM were added in 5 μl for a final concentration of 20 μM and 10 μM, respectively. Plates were incubated 15 min and visualized by eye or imaged using the automated microscope. Compounds that showed an increase in the percentage of cells stained with ethidium bromide were noted as toxic.

Immunofluorescence

Cells were fixed as described for screening plates above. Coverslips were blocked in TBS-Tx containing 2% BSA (AbDil) for 30 min; antibodies diluted in AbDil were incubated for 45 min, washed 3 times with TBS-Tx, incubated for 45 min with secondary antibodies in AbDil, washed 3 times with TBS-Tx, 1 time with water; and mounted in mounting media (0.5% p-phenylenediamine in 20 mM Tris [pH 8.8], 90% glycerol). Antibodies and stains used: filaman (Oncogene Research Products CP72), α-actinin (Sigma A5044), ezrin (Sigma E8897), vinculin (Sigma V9131).

M2 Cell Blebbing Assay

M2 cells were split into 12-well plates containing 10 mm coverslips. After 2 hr, compounds were added to wells for 2 or 10 min. Cells were fixed for 10 min with the addition of an equivalent volume of media containing 8% formaldehyde. Cells were washed with TBS-Tx, stained with 0.5 μg/ml TMR NHS-ester (Molecular Probes C-1171) for 10 min, washed with TBS-Tx, incubated with 1 μg/ml Hoechst for 2 min (found to be necessary for uniform NHS-ester staining, possibly by quenching any remaining NHS-ester), washed 2 times with TBS-Tx, and mounted.

Cell Signaling by Western Blotting

M2 and Balb3T3 cells were plated in 6-well plates at 80% confluency. Cells were starved overnight in their respective media with 0.1% FBS. Compounds were added to wells and incubated for 10 min before the addition of 10%–20% FBS in experiments involving stimulation. After an additional 10 min, media was removed and 300 μl of Laemmli sample buffer was added. Samples were boiled for 2 min, and sonicated before loading on SDS PAGE gels. Standard Western blotting techniques were used. Antibodies used: phospho-myosin light chain 2 Ser19 (Cell Signaling 3671), phospho-Akt Ser473 (Cell Signaling 9271), GAPDH (US Biological G8140-01), 4G10 (Upstate 16-204), and phospho-ERM (Cell Signaling 3141).

Activated Rho Pull-Down Assays

Balb3T3 cells were plated, starved, and treated with compounds as above. After 5 min in the presence or absence of 20% serum, media was replaced by 300 μl of 1× PBD (50 mM Tris-HCl [pH 7.5], 10 mM MgCl2, 200 mM NaCl, 1% IGEPAL, and 5% glycerol), cells were scrape collected and Rhotekin RBD pull-down assays were performed as described [32]. Immunoprecipitate was separated by electrophoresis (12% SDS-PAGE) and blots were probed with RhoA antibody (Santa Cruz sc-418).

MLCK Kinase Assay

Myosin light chain kinase activity was assayed in MLCK buffer (50 mM Tris [pH 7.0], 100 mM KCl, 10 mM MgCl2, 0.2 mM CaCl2, and 1 mM DTT). Each reaction contained 1 μg human platelet myosin, 0.125 μg calmodulin, and 38 ng MLCK. Reactions were mixed with indicated concentrations of inhibitor, then ATP was added to give a final concentration of 30 μM cold ATP and 1.5 μM g-32P-ATP (10 Ci/mmol). Reactions were incubated for 10 min at 30°C, stopped by the addition Laemmli sample buffer, and separated by SDS-PAGE (15%).

ROCK Kinase Assay

ROCK activity was assayed with purified GST-ROCK catalytic domain kindly provided by K. Kaibuchi [29]. Kinase assays were performed at 30°C for 20 min (unless otherwise noted) with 150 ng of ROCK in 30 μl of buffer (20 mM Tris [pH 7.5], 50 mM NaCl, 5 mM $MgCl_2$, and 1 mM DTT) with 0.1 mM ATP, 0.1 μM g-32P-ATP (0.1 mCi/ml), and 3 μg myelin basic protein. Samples were run on 15% SDS-PAGE gels, dried, and exposed to a phosphorimager screen. Gel bands were quantified with Quantity One software (BioRad).

Kinase Specificity

ROCK-II(h), PRK2(h), MSK1(h), and PKA(h) were chosen based on results that all or some are inhibited by the ROCK inhibitors Y-27632, H89, and HA1077 while PKC(α)(h), and SAPK2a(h) do not show inhibition by these compounds [34]. A Kinase Profiler assay (Upstate Biotechnology) was performed in duplicate with 25 μM FKAF, 100 μM ATP, and assay conditions detailed at (http://www.upstate.com/img/pdf/kp_protocols_full.pdf). Data is plotted as average and range/√2.

Screening of Compounds with Known Bioactivities

Compound plates (ICCB Bioactives 1, http://iccb.med.harvard.edu/screening/compound_libraries/bioactives_collection1.htm) for each concentration were assembled from dry and liquid stocks by members of the ICCB screening room. Three concentrations were made: high, 5 mg/ml; medium, 1.1 mg/ml; and low, 0.25 mg/ml with exceptions made to accommodate extremely potent or nonpotent compounds. BS-C-1 were plated in 40 μl after we pin transferred 100 nl from each compound plate. Compounds were screened in duplicate in the 7 hr wound healing assay and fixed, stained, and imaged as before. The complete data set including images is available upon request. Bioactivities were compiled from Pubmed citations, as well as Calbiochem, BioMol, and Tocris catalogs.

Acknowledgments

We'd like to thank Mimi Shirasu-Hiza for critical reading and great help with the manuscript. She and other members of the Mitchison lab provided stimulating discussion and help. We'd like to thank Terry Lechler for help with the permeabilized yeast assay, Aaron Straight for the kind gift of the reagents required for the MLCK assays, K. Kaibuchi for purified ROCK, and Fumio Matsumura for putting us in contact with G.T. Angie Martinez and Sheri Moores were very helpful with all things Western. Thanks as well to E.W., T.C., J.E., and R.Y. for naming the compound. The authors have no financial conflict of interest associated with this work. Support was provided to J.Y. by an HHMI predoctoral fellowship, to G.C. by a Wellcome Trust Overseas fellowship, and to T.J.M. by NIH GM62566.

Received: August 27, 2004
Revised: December 31, 2004
Accepted: January 4, 2005
Published: March 25, 2005

References

1. Uehata, M., Ishizaki, T., Satoh, H., Ono, T., Kawahara, T., Morishita, T., Tamakawa, H., Yamagami, K., Inui, J., Maekawa, M., et al. (1997). Calcium sensitization of smooth muscle mediated by a Rho-associated protein kinase in hypertension. Nature *389*, 990–994.
2. Wani, M.C., Taylor, H.L., Wall, M.E., Coggon, P., and McPhail, A.T. (1971). Plant antitumor agents. VI. The isolation and struc-

ture of taxol, a novel antileukemic and antitumor agent from Taxus brevifolia. J. Am. Chem. Soc. *93*, 2325–2327.
3. Kashman, Y., Groweiss, A., and Shmueli, U. (1980). Latrunculin, a new 2-thiazolidinone macrolide from the marine pponge Latrunculia magnificia1. Tetrahedron Lett. *21*, 3629–3632.
4. Feng, Y., Yu, S., Lasell, T.K., Jadhav, A.P., Macia, E., Chardin, P., Melancon, P., Roth, M., Mitchison, T., and Kirchhausen, T. (2003). Exo1: a new chemical inhibitor of the exocytic pathway. Proc. Natl. Acad. Sci. USA *100*, 6469–6474.
5. Mayer, T.U., Kapoor, T.M., Haggarty, S.J., King, R.W., Schreiber, S.L., and Mitchison, T.J. (1999). Small molecule inhibitor of mitotic spindle bipolarity identified in a phenotype-based screen. Science *286*, 971–974.
6. Kau, T.R., Schroeder, F., Ramaswamy, S., Wojciechowski, C.L., Zhao, J.J., Roberts, T.M., Clardy, J., Sellers, W.R., and Silver, P.A. (2003). A chemical genetic screen identifies inhibitors of regulated nuclear export of a Forkhead transcription factor in PTEN-deficient tumor cells. Cancer Cell *4*, 463–476.
7. Mitchison, T.J. (1994). Towards a pharmacological genetics. Chem. Biol. *1*, 3–6.
8. Taylor, D.L., Woo, E.S., and Giuliano, K.A. (2001). Real-time molecular and cellular analysis: the new frontier of drug discovery. Curr. Opin. Biotechnol. *12*, 75–81.
9. Abraham, V.C., Taylor, D.L., and Haskins, J.R. (2004). High content screening applied to large-scale cell biology. Trends Biotechnol. *22*, 15–22.
10. Yarrow, J.C., Feng, Y., Perlman, Z.E., Kirchhausen, T., and Mitchison, T.J. (2003). Phenotypic screening of small molecule libraries by high throughput cell imaging. Comb. Chem. High Throughput Screen. *6*, 279–286.
11. Yarrow, J.C., Perlman, Z.E., Westwood, N.J., and Mitchison, T.J. (2004). A high-throughput cell migration assay using scratch wound healing, a comparison of image-based readout methods. BMC Biotechnol. *4*, 21.
12. Seppa, H., Grotendorst, G., Seppa, S., Schiffmann, E., and Martin, G.R. (1982). Platelet-derived growth factor in chemotactic for fibroblasts. J. Cell Biol. *92*, 584–588.
13. Pierce, G.F., Mustoe, T.A., Lingelbach, J., Masakowski, V.R., Griffin, G.L., Senior, R.M., and Deuel, T.F. (1989). Platelet-derived growth factor and transforming growth factor-beta enhance tissue repair activities by unique mechanisms. J. Cell Biol. *109*, 429–440.
14. Lipinski, C., Lombardo, F., Dominy, B., and Feeney, P. (1997). Experimental and computational approaches to estimate solubility and permeability in drug discovery and development settings. Adv. Drug Deliv. Rev. *23*, 3–25.
15. Peterson, J.R., Lokey, R.S., Mitchison, T.J., and Kirschner, M.W. (2001). A chemical inhibitor of N-WASP reveals a new mechanism for targeting protein interactions. Proc. Natl. Acad. Sci. USA *98*, 10624–10629.
16. Peterson, J.R., Bickford, L.C., Morgan, D., Kim, A.S., Ouerfelli, O., Kirschner, M.W., and Rosen, M.K. (2004). Chemical inhibition of N-WASP by stabilization of a native autoinhibited conformation. Nat. Struct. Mol. Biol. *11*, 747–755.
17. Hotha, S., Yarrow, J.C., Yang, J.G., Garrett, S., Renduchintala, K.V., Mayer, T.U., and Kapoor, T.M. (2003). HR22C16: a potent small-molecule probe for the dynamics of cell division. Angew. Chem. Int. Ed. Engl. *42*, 2379–2382.
18. Cunningham, C.C., Gorlin, J.B., Kwiatkowski, D.J., Hartwig, J.H., Janmey, P.A., Byers, H.R., and Stossel, T.P. (1992). Actin-binding protein requirement for cortical stability and efficient locomotion. Science *255*, 325–327.
19. Mills, J.C., Stone, N.L., Erhardt, J., and Pittman, R.N. (1998). Apoptotic membrane blebbing is regulated by myosin light chain phosphorylation. J. Cell Biol. *140*, 627–636.
20. Coleman, M.L., Sahai, E.A., Yeo, M., Bosch, M., Dewar, A., and Olson, M.F. (2001). Membrane blebbing during apoptosis results from caspase-mediated activation of ROCK I. Nat. Cell Biol. *3*, 339–345.
21. Sebbagh, M., Renvoize, C., Hamelin, J., Riche, N., Bertoglio, J., and Breard, J. (2001). Caspase-3-mediated cleavage of ROCK I induces MLC phosphorylation and apoptotic membrane blebbing. Nat. Cell Biol. *3*, 346–352.
22. Straight, A.F., Cheung, A., Limouze, J., Chen, I., Westwood, N.J., Sellers, J.R., and Mitchison, T.J. (2003). Dissecting temporal and spatial control of cytokinesis with a myosin II inhibitor. Science *299*, 1743–1747.
23. Song, Y., Hoang, B.Q., and Chang, D.D. (2002). ROCK-II-induced membrane blebbing and chromatin condensation require actin cytoskeleton. Exp. Cell Res. *278*, 45–52.
24. Hirose, M., Ishizaki, T., Watanabe, N., Uehata, M., Kranenburg, O., Moolenaar, W.H., Matsumura, F., Maekawa, M., Bito, H., and Narumiya, S. (1998). Molecular dissection of the Rho-associated protein kinase (p160ROCK)-regulated neurite remodeling in neuroblastoma N1E–115 cells. J. Cell Biol. *141*, 1625–1636.
25. Sahai, E., Ishizaki, T., Narumiya, S., and Treisman, R. (1999). Transformation mediated by RhoA requires activity of ROCK kinases. Curr. Biol. *9*, 136–145.
26. Kanthou, C., and Tozer, G.M. (2002). The tumor vascular targeting agent combretastatin A-4-phosphate induces reorganization of the actin cytoskeleton and early membrane blebbing in human endothelial cells. Blood *99*, 2060–2069.
27. Narumiya, S., Ishizaki, T., and Uehata, M. (2000). Use and properties of ROCK-specific inhibitor Y-27632. Methods Enzymol. *325*, 273–284.
28. Matsui, T., Amano, M., Yamamoto, T., Chihara, K., Nakafuku, M., Ito, M., Nakano, T., Okawa, K., Iwamatsu, A., and Kaibuchi, K. (1996). Rho-associated kinase, a novel serine/threonine kinase, as a putative target for small GTP binding protein Rho. EMBO J. *15*, 2208–2216.
29. Amano, M., Ito, M., Kimura, K., Fukata, Y., Chihara, K., Nakano, T., Matsuura, Y., and Kaibuchi, K. (1996). Phosphorylation and activation of myosin by Rho-associated kinase (Rho-kinase). J. Biol. Chem. *271*, 20246–20249.
30. Kimura, K., Ito, M., Amano, M., Chihara, K., Fukata, Y., Nakafuku, M., Yamamori, B., Feng, J., Nakano, T., Okawa, K., et al. (1996). Regulation of myosin phosphatase by Rho and Rho-associated kinase (Rho-kinase). Science *273*, 245–248.
31. Maekawa, M., Ishizaki, T., Boku, S., Watanabe, N., Fujita, A., Iwamatsu, A., Obinata, T., Ohashi, K., Mizuno, K., and Narumiya, S. (1999). Signaling from Rho to the actin cytoskeleton through protein kinases ROCK and LIM-kinase. Science *285*, 895–898.
32. Ren, X.D., Kiosses, W.B., and Schwartz, M.A. (1999). Regulation of the small GTP-binding protein Rho by cell adhesion and the cytoskeleton. EMBO J. *18*, 578–585.
33. Ishizaki, T., Uehata, M., Tamechika, I., Keel, J., Nonomura, K., Maekawa, M., and Narumiya, S. (2000). Pharmacological properties of Y-27632, a specific inhibitor of rho-associated kinases. Mol. Pharmacol. *57*, 976–983.
34. Davies, S.P., Reddy, H., Caivano, M., and Cohen, P. (2000). Specificity and mechanism of action of some commonly used protein kinase inhibitors. Biochem. J. *351*, 95–105.
35. Hann, M.M., and Oprea, T.I. (2004). Pursuing the leadlikeness concept in pharmaceutical research. Curr. Opin. Chem. Biol. *8*, 255–263.
36. Oprea, T.I. (2002). Current trends in lead discovery: are we looking for the appropriate properties? J. Comput. Aided Mol. Des. *16*, 325–334.
37. Hu, E., and Lee, D. (2003). Rho kinase inhibitors as potential therapeutic agents for cardiovascular diseases. Curr. Opin. Investig. Drugs *4*, 1065–1075.
38. Hattori, T., Shimokawa, H., Higashi, M., Hiroki, J., Mukai, Y., Tsutsui, H., Kaibuchi, K., and Takeshita, A. (2004). Long-term inhibition of Rho-kinase suppresses left ventricular remodeling after myocardial infarction in mice. Circulation *109*, 2234–2239.
39. May, R.C., and Machesky, L.M. (2001). Phagocytosis and the actin cytoskeleton. J. Cell Sci. *114*, 1061–1077.
40. Uff, C.R., Pockley, A.G., and Phillips, R.K. (1993). A rapid microplate-based fluorometric assay for phagocytosis. Immunol. Invest. *22*, 407–413.
41. Li, R., Zheng, Y., and Drubin, D.G. (1995). Regulation of cortical actin cytoskeleton assembly during polarized cell growth in budding yeast. J. Cell Biol. *128*, 599–615.
42. Lechler, T., and Li, R. (1997). In vitro reconstitution of cortical actin assembly sites in budding yeast. J. Cell Biol. *138*, 95–103.
43. Brieher, W.M., Coughlin, M., and Mitchison, T.J. (2004). Fascin-mediated propulsion of Listeria monocytogenes independent of frequent nucleation by the Arp2/3 complex. J. Cell Biol. *165*, 233–242.